



ELSEVIER

Contents lists available at ScienceDirect

Physica B

journal homepage: www.elsevier.com/locate/physb

Doping effects on the magnetic properties of NdRhIn₅ intermetallic antiferromagnet

R. Lora-Serrano^{a,b,*}, D.J. Garcia^{a,c}, E. Miranda^a, C. Adriano^a, L. Bufaiçal^a, J.G.S. Duque^a, P.G. Pagliuso^a

^a Instituto de Física “Gleb Wataghin”, UNICAMP, 13083-970 Campinas-São Paulo, Brazil

^b Instituto de Física, Universidade Federal de Uberlândia, 38400-902 Uberlândia-MG, Brazil

^c Consejo Nacional de Investigaciones Científicas y Técnicas (CONICET) and Centro Atómico Bariloche, S.C. de Bariloche, Río Negro, Argentina

ARTICLE INFO

PACS:
75.50.Ee
75.10.Dg
75.30.Kz

Keywords:
Antiferromagnetics
Crystal-field theory and spin Hamiltonians
Magnetic phase boundaries

ABSTRACT

We report temperature dependent heat capacity and magnetization measurements on single crystals of Nd_{1-x}La_xRhIn₅ ($x = 0.15, 0.4$ and 0.5) and NdRhIn_{5-x}Sn_x ($x = 0.08, 0.12$ and 0.24). NdRhIn₅ is an antiferromagnetic (AFM) compound with $T_N \approx 11$ K which crystallizes in the same layered tetragonal structure of the CeMIn₅ family ($M = \text{Rh, Co and Ir}$), where different ground states can be found by tuning the interplay among different microscopic interactions such as the Kondo effect, crystal field (CEF) effects and the Ruderman–Kittel–Kasuya–Yoshida (RKKY) magnetic interaction. Here, we explore the evolution of the AFM correlations in this Nd-based (non-Kondo) compound while perturbing the RKKY exchange by using two different substitutions: (i) replacing Nd³⁺ by non-magnetic La³⁺ within NdIn₃ atomic planes (dilution) and (ii) substituting In by Sn in the In-sites (electronic tuning). For both types of doping, our results show the suppression of the AFM state as the La- or Sn-content is increased. This doping induced suppression of the AFM order is discussed considering the effects of dilution and effects in the tetragonal CEF using a mean-field model applied to the observed data. Our results are compared to the properties of other members of the RRhIn₅ family considering the role of dimensionality in the magnetic interactions.

© 2009 Elsevier B.V. All rights reserved.

1. Introduction

Dilution in magnetically ordered system is one of the important subjects within the study of percolation phenomena. It represents a way to understand the nature of long and short range antiferromagnetic (AFM) ordering in strongly correlated electrons systems, where it might be used to suppress the Néel state and probe interesting different ground states near to the AFM quantum critical point (QCP). In this regard, a series intensively investigated in the last eight years is the family of heavy-fermion superconductors CeMIn₅ ($M = \text{Rh, Co, Ir}$), where magnetic dilution by chemical doping has proved to be a valuable tool as tuning parameter in the interplay between the Kondo effect and the long range Ruderman–Kittel–Kasuya–Yoshida (RKKY) magnetic interaction. The balance between these two interactions as a function of doping may tune the ground state of a system from heavy-fermion paramagnetic metal or unconventional superconductors to a long range ordered AFM state [1–10].

Recently, La- and Sn-doping studies on CeRhIn₅ under pressure were reported [11]. These results performed on single crystals of

Ce_{0.9}La_{0.1}RhIn₅ and CeRhIn_{4.84}Sn_{0.16} have shown that although both compounds have the same $T_N = 2.8$ K, Sn-doping shifts the pressure induced superconducting phase to lower pressures (compared to those required in the undoped CeRhIn₅) while La-doping does exactly the opposite, shifting the P – T phase diagram to higher pressure. These observations reveal that the strength of the Kondo coupling is the relevant energy scale to set the pressure range for the occurrence of superconductivity (SC) in CeRhIn₅ [11]. These results indicate that one important step to understand the doped-induced evolution of the physical properties of the Ce-based RMIn₅ family may be the analysis of dilution effects on the magnetic interaction between rare earth ions in non-Kondo isostructural materials from the $R_mM_n\text{In}_{3m+2n}$ ($R = \text{Ce–La}$; $M = \text{Co, Rh or Ir}$; $m = 1, 2$; $n = 0, 1$) family, where the absence of strong hybridization between the localized 4f electrons and the conduction 5d electrons make them a reference compounds to study the suppression of antiferromagnetism in these series. Our recent work on Tb_{1-x}La_xRhIn₅ ($0.0 < x < 1.0$) [12], where we evaluated the role of the different mechanisms for the suppression of the long-range AFM coupling by considering dilution, changes in the CEF scheme and the introduction of disorder is a relevant example on the subject. In Tb_{1-x}La_xRhIn₅ series, the Néel temperature decreases with a non-linear behavior as a function of La-concentration and extrapolates to zero at

* Corresponding author. Tel./fax: +55 34 32394081.

E-mail address: rloraserrano@infis.ufu.br (R. Lora-Serrano).

roughly 70% of La content (the site percolation threshold for a 3D magnetic system), differently to the $x_c \sim 40\%$ observed for $\text{Ce}_{1-x}\text{La}_x\text{RhIn}_5$ and $(\text{Ce}_{1-x}\text{La}_x)_2\text{RhIn}_8$ families. X-ray magnetic scattering experiments for the determination of magnetic structure on a sample with 40% of La-content revealed that the magnetic wave vector is the same as for the undoped compound. Also, it was concluded that the crystal field scheme evolves as a function of La-doping and affects T_N as much as the decreasing in J_{RKKY} due to dilution [12]. In NdRhIn_5 compound, which is also an isostructural non-Kondo member of the CeMIn_5 heavy-fermion series and orders antiferromagnetically below $T_N \sim 11$ K, Nd^{3+} ($J = \frac{9}{2}$) is a Krammer ion such as Ce^{3+} ($J = \frac{5}{2}$) and the CEF effects act in distinct way than that for Tb^{3+} ($J = 6$) which is a non-Krammer ion. As such, dilution studies on NdRhIn_5 may represent an interesting complementary study to the dilution studies on TbRhIn_5 [12]. In this work, we have explored the doping effects on the magnetic interactions between Nd^{3+} ions by two different chemical substitutions: replacing Nd^{3+} by non-magnetic La^{3+} ions for $0 \leq x \leq 0.5$, and substituting In by Sn for $x = 0, 0.08, 0.12, 0.24$ and 0.48 . The doping evolution of the magnetic properties of NdRhIn_5 was studied by measuring magnetic susceptibility and specific heat as a function of temperature. The reported data was interpreted considering the doping effects on the long-range AFM RKKY interaction and on the CEF scheme as a function of dopant concentration in both series.

2. Experimental results and discussion

Single crystals of $\text{Nd}_{1-x}\text{La}_x\text{RhIn}_5$ ($x = 0, 0.15, 0.3, 0.4$ and 0.5) and $\text{NdRhIn}_{5-x}\text{Sn}_x$ ($x = 0, 0.08, 0.12, 0.24$ and 0.48) were grown by the self-flux method [13]. In the case of the $\text{Nd}_{1-x}\text{La}_x\text{RhIn}_5$ series, x denotes the nominal concentration of Lanthanum. For $\text{NdRhIn}_{5-x}\text{Sn}_x$ compounds, the starting materials were mixed in the ratio Nd:Rh:In:Sn = 1:1:20y, and x was taken as $x \sim 0.4y$ as in the case of CeRhIn_5 [7]. The grown single crystals were confirmed by powder X-ray diffraction to crystallize in the HoCoGa_5 -type structure with no traces of the Nd_2RhIn_8 or NdIn_3 phases. For the magnetic characterization of both systems, magnetization measurements were performed in a commercial SQUID magnetometer at $H = 1$ kOe in the temperature range between 2 and 300 K. Specific heat measurements were performed in a quantum design PPMS small-mass calorimeter that employs a quasi-adiabatic thermal relaxation technique; C/T data were taken between $1.8 \leq T \leq 40$ K.

The first observed effect from the introduction of the larger La^{3+} ion in the NdRhIn_5 structure is the linear increase of the tetragonal cell parameters, a and c (Fig. 1), in agreement with the Vegard's law for solid solutions. a and c were determined from least-squares minimization of the Bragg peak positions (2θ) [14]. For $\text{NdRhIn}_{5-x}\text{Sn}_x$, our X-ray powder diffraction patterns and cell parameters calculations revealed that there are no appreciable changes in the lattice parameters within the Sn-concentration range. Horizontal error bars in Fig. 1 has been estimated from linear fits to the inverse of the magnetic susceptibility for $T > 200$ K and assuming the full calculated moment of $3.66\mu_B$ for the free Nd^{3+} ion. Vertical error bars are extracted from the cell parameters calculations.

In Fig. 2 we show the results of the macroscopic measurements (magnetic susceptibility and specific heat) of three representative samples from each studied family. The three panels to the left contain the data of the $\text{Nd}_{1-x}\text{La}_x\text{RhIn}_5$ ($x = 0, 0.15$ and 0.4) series while the ones to the right show the data for $\text{NdRhIn}_{5-x}\text{Sn}_x$ ($x = 0, 0.12$ and 0.24) samples. Data for NdRhIn_5 taken from Ref. [15] were also included. For all cases, the main panels depict the data of magnetic susceptibilities for $H = 1$ kOe applied parallel (χ_{\parallel}) and

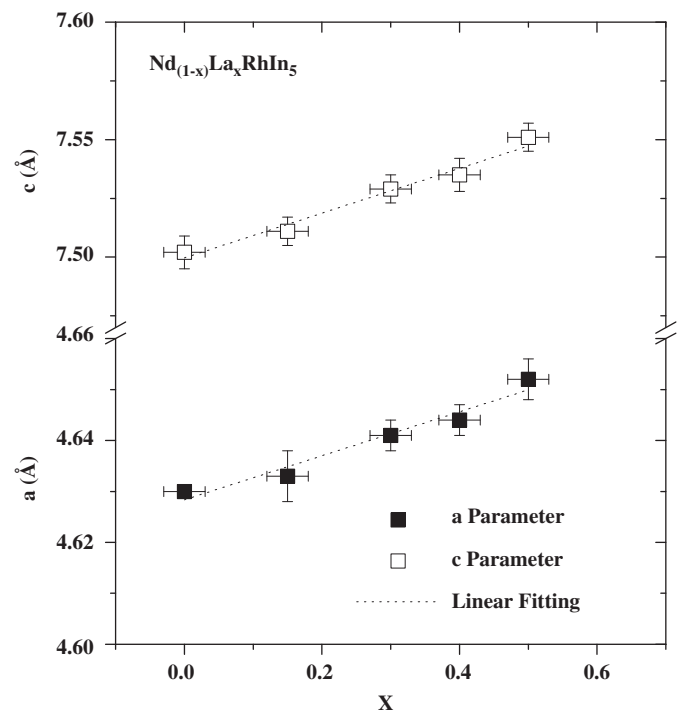


Fig. 1. Cell parameters of $\text{Nd}_{1-x}\text{La}_x\text{RhIn}_5$ ($x = 0, 0.15, 0.3, 0.4, 0.5$) as a function of x .

perpendicular (χ_{\perp}) to the c -axis, while the insets contain the specific heat data. The solid curves represent the best fits to the experimental data using the mean field (MF) model of Ref. [16] which includes a mean field first-neighbors exchange interaction and the tetragonal CEF Hamiltonian. The temperature of the maximum in both $\chi(T)$ and C/T curves coincides well and we have taken these temperature values as the Néel temperature T_N .

From our $\chi(T)$ and C/T , becomes evident the shift of T_N to lower- T as the doping content is increased, indicating the weakening of long range magnetic correlations between Nd^{3+} ions as La or Sn atoms enter the structure. The broadening of the transition in the T_N data is more evident for the La-doped samples than for the Sn-doped ones, which is consistent with a smaller dilution limit in the former compounds (see below). Interesting, the MF simulations in both cases follow the details of the experimental data quite well, which is indicative of the evolution of CEF effects as a function of doping.

In Fig. 3 we present the x -dependence of the normalized Néel temperature ($T_{N,x}/T_{N,x=0}$) as extracted from the data of Fig. 2 for all the La-doped (filled circles) and Sn-doped (open circles) studied samples. Additionally, we show the reported T_N values from the series $\text{CeRhIn}_{5-x}\text{Sn}_x$ [7] (open diamonds), $\text{Ce}_{1-x}\text{La}_x\text{RhIn}_5$ [4] (filled diamonds) and $\text{Tb}_{1-x}\text{La}_x\text{RhIn}_5$ [12] (stars) for comparison. For both Ce-based families, T_N shows a linear decrease (dashed lines) as a function of x . This is also the case for the $\text{NdRhIn}_{5-x}\text{Sn}_x$ compounds, while a non-linear (the dashed-dotted curves) T_N suppression as a function of x is found in $\text{Nd}_{1-x}\text{La}_x\text{RhIn}_5$ and $\text{Tb}_{1-x}\text{La}_x\text{RhIn}_5$. For the $\text{Nd}_{1-x}\text{La}_x\text{RhIn}_5$ series, we observed no long range order for $x = 0.5$, thus the critical concentration at which $T_N \rightarrow 0$ must be between $0.4 < x_c < 0.5$, roughly the same x_c found in the $\text{Ce}_{1-x}\text{La}_x\text{RhIn}_5$ ($x_c \sim 0.4$) [4]. However, above $x = 0.3$, T_N suddenly drops to zero with a non-linear behavior, contrasting with the linear decrease observed in Ce-based materials. For $\text{Tb}_{1-x}\text{La}_x\text{RhIn}_5$, the same evolution has been observed with a higher dilution limit of $0.7 < x_c < 0.8$ [12]. For $\text{NdRhIn}_{5-x}\text{Sn}_x$ compounds, on the other hand, we could not determine, in this work, the dilution limit up to the higher studied concentration

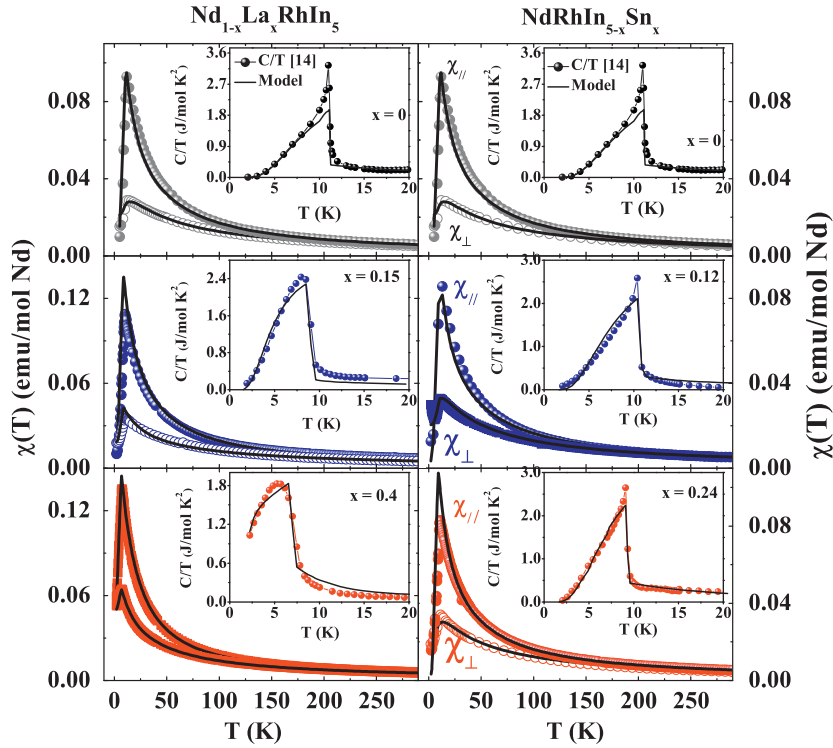


Fig. 2. (Color online) Temperature dependence of the magnetic susceptibility, $\chi(T)$ (main panels) and specific heat, $C/T(T)$, (insets) for $\text{Nd}_{1-x}\text{La}_x\text{RhIn}_5$ ($x = 0, 0.15$ and 0.4)—left, from top to bottom—and $\text{NdRhIn}_{5-x}\text{Sn}_x$ ($x = 0, 0.12$ and 0.24)—right, from top to bottom—compounds. Solid curves are the best fits to the data using the mean field model of Ref. [16].

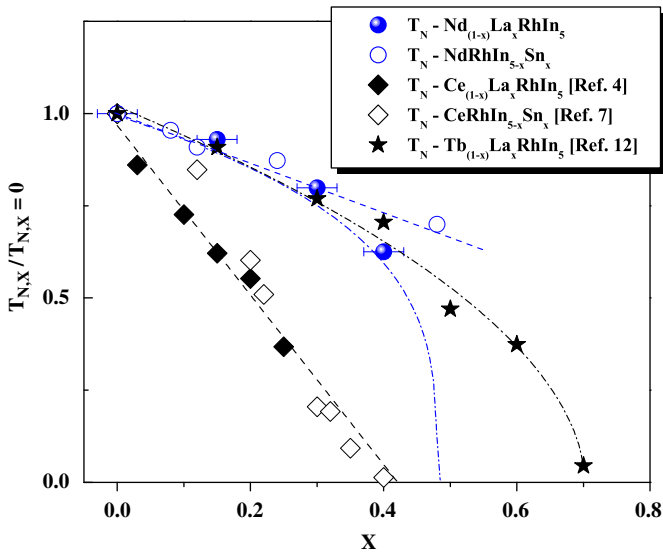


Fig. 3. (Color online) Normalized Néel temperature ($T_{N,x}/T_{N(x=0)}$) vs. x for $\text{Nd}_{1-x}\text{La}_x\text{RhIn}_5$ (closed circles) and $\text{NdRhIn}_{5-x}\text{Sn}_x$ (open circles) extracted from $C/T(T)$ and $\chi(T)$ data. The $\text{Ce}_{1-x}\text{La}_x\text{RhIn}_5$ (closed diamonds) and $\text{CeRhIn}_{5-x}\text{Sn}_x$ (open diamonds) data taken from Refs. [4,7], as well as the data of $\text{Tb}_{1-x}\text{La}_x\text{RhIn}_5$ (star symbols) from Ref. [12] are included for comparison. Dashed and dotted lines represent linear and power-law fits, respectively, to all data sets.

($x = 0.48$). However, our results suggests that T_N decreases less dramatically in $\text{NdRhIn}_{5-x}\text{Sn}_x$ than in their $\text{CeRhIn}_{5-x}\text{Sn}_x$ relatives, where $x_c \sim 0.35$ (roughly the same of $\text{Ce}_{1-x}\text{La}_x\text{RhIn}_5$) [7].

For our doped samples of NdRhIn_5 , the long range order suppression may result from combined effects. For $\text{Nd}_{1-x}\text{La}_x\text{RhIn}_5$, the dilution effect and the unit cell volume expansion as La^{3+} substitutes Nd^{3+} (Fig. 1) are important factors to be considered as they increase the average distance between the remaining Nd^{3+}

ions and tends to diminish the J_{RKKY} exchange between them. However, for $\text{NdRhIn}_{5-x}\text{Sn}_x$, the previous two effects are not present since the Nd^{3+} concentration and the unit cell parameters do not change as a function of Sn-doping for the studied concentrations. In this case, when Sn replaces In, there may be a local increase of the density of states as Sn introduces a p electron at the replaced In site. For $\text{CeRhIn}_{5-x}\text{Sn}_x$, it has been shown that this electronic tuning enhances the exchange interaction between the 4f electrons and the conduction electrons, J_{fs} , leading to an increasing of the Kondo coupling and a consequent T_N suppression [7]. On other hand, for $\text{NdRhIn}_{5-x}\text{Sn}_x$, considering only the increase of J_{fs} , one should expect an enhanced T_N due to the consequent increase of J_{RKKY} and the absence of Kondo effect. Therefore, the T_N suppression in Sn-doped compounds should have other microscopic origin.

It is interesting to notice that the local electronic tuning caused by the Sn-doping also may affect the charge distribution at a nearby Nd^{3+} site, modifying the CEF effects. This effect also occurs with La-doping at the Nd^{3+} site, where small differences in ionic size between La^{3+} and Nd^{3+} still induce a chemical pressure on the lattice and perturb the CEF wave function. In fact, the evolution the CEF scheme as function of doping for the studied samples is presented in Fig. 4 where we show the scheme of energy levels (in Kelvins) for representative samples of $\text{Nd}_{1-x}\text{La}_x\text{RhIn}_5$ ($x = 0, 0.15$ and 0.4 , left panel) and $\text{NdRhIn}_{5-x}\text{Sn}_x$ ($x = 0, 0.12$ and 0.24 , right panel) intermetallic compounds. These CEF schemes were extracted using the MF simulations of the data of Fig. 2.

It can be observed that the scheme formed by a ground-state doublet with four excited doublets evolves by changing the energy separation between these doublets as a function dopant concentration. For Sn-doping there is a clear decrease of the overall splitting as a function of doping, suggesting a direct relationship between the decrease of both T_N and the doublets-doublets energy splitting. For La-doping, CEF energy levels

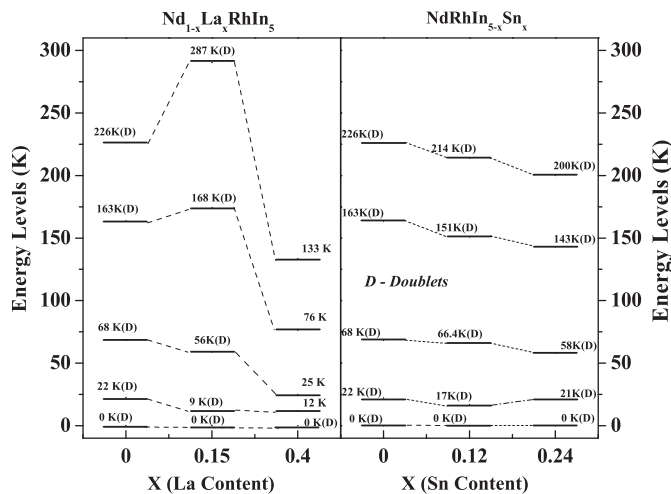


Fig. 4. CEF splitting of the Nd ground state multiplets obtained from the simulations of Fig. 2 to the $\text{Nd}_{1-x}\text{La}_x\text{RhIn}_5$ ($x = 0, 0.15$ and 0.4)—left panel—and to the $\text{NdRhIn}_{5-x}\text{Sn}_x$ ($x = 0, 0.12$ and 0.24)—right panel—using the MF model of Ref. [16].

shows a non-monotonic evolution for $T > 150\text{K}$, but also shows a decrease of the splitting for the low- T scheme of levels. These results indicate that the doping effects on the CEF levels scheme should be taken into account to understand the evolution of T_N and other important energy scales in these series and related materials.

Concerning the dilution limit in La-doped series, it is mainly determined by the dimensionality of Nd^{3+} – Nd^{3+} interactions. It has been shown that the c/a ratio of the cell parameters along the RRhIn_5 family decreases accompanying the decrease of the rare earth ionic radii [17,18]. Therefore, the smaller value of $x_c \sim 0.45$ for $\text{Nd}_{1-x}\text{La}_x\text{RhIn}_5$ as compared to $x_c \sim 0.7$ found in the Tb-based series, might be explained in terms of the smaller 3D character of the $J_{\text{Nd-Nd}}$ exchange. In other words, within the $\text{Nd}_{1-x}\text{La}_x\text{RhIn}_5$ family compounds the character of magnetic interactions are more dimensionally closer to the $\text{Ce}_{1-x}\text{La}_x\text{RhIn}_5$ family and to the percolation threshold (where $x_c \sim 0.40$) [4,19]. Nonetheless, there is a non-linear suppression of T_N for the $\text{Nd}_{1-x}\text{La}_x\text{RhIn}_5$ compounds that should be related to the complexity of the percolation in the dilution limit of systems with long range magnetic exchange, as the damped RKKY interaction. Indeed, the behavior of a diluted system close to x_c is very similar to the critical behavior near a continuous (second order) phase transition with geometric fluctuations, where doping in the former plays the role of the usual thermal or quantum fluctuations in the later. This implies that observables (e.g. T_N) are governed by

power-law scaling relations [20,21]. A discussion about the values of the critical exponents, as well as the universality class of these families, will be addressed in future works.

3. Conclusions

We have reported the results of the low temperature magnetic properties of La- and Sn-doped NdRhIn_5 antiferromagnetic compounds. T_N decreases with a non-linear behavior as a function of the Lanthanum concentration for $\text{Nd}_{1-x}\text{La}_x\text{RhIn}_5$ and extrapolates to zero at roughly 45% of La content, differently from their structural-related $\text{Tb}_{1-x}\text{La}_x\text{RhIn}_5$ ($x_c \sim 70\%$) and roughly the same of the $\text{Ce}_{1-x}\text{La}_x\text{RhIn}_5$ family, where $x_c \sim 40\%$ (the theoretical site percolation threshold for a 2D diluted magnet). Doping with Sn in $\text{NdRhIn}_{5-x}\text{Sn}_x$ dilutes the system much slower than for the La-doping case and we still cannot define a critical concentration for the highest concentration studied ($x = 0.48$). Our magnetization and specific heat data have been successfully simulated with our mean field model and the analysis revealed doping-induced effects on the CEF scheme for both series.

Acknowledgments

This work was supported by FAPESP-SP and CNPq (Brazil).

References

- [1] A. Schroeder, et al., *Internat. J. Mod. Phys. B* 16 (2002) 3031.
- [2] P.G. Pagliuso, et al., *Phys. Rev. B* 64 (2001) 100503 (R).
- [3] P.G. Pagliuso, et al., *Physica B* 312–313 (2002) 129.
- [4] P.G. Pagliuso, et al., *Phys. Rev. B* 66 (2002) 054433.
- [5] L.D. Pham, et al., *Phys. Rev. Lett.* 97 (2006) 056404.
- [6] E.D. Bauer, et al., *Phys. Rev. Lett.* 94 (2005) 047001.
- [7] E.D. Bauer, et al., *Physica B* 378–380 (2006) 142.
- [8] V.S. Zapf, et al., *Phys. Rev.* 65 (2002) 014506.
- [9] N.O. Moreno, et al., *Physica B* 312–313 (2002) 274.
- [10] M. Nicklas, et al., *Phys. Rev. B* 70 (2004) 020505 (R).
- [11] L. Mendonça Ferreira, et al., *Phys. Rev. Lett.* 101 (2008) 017005.
- [12] R. Lora-Serrano, et al., *Phys. B* 79 (2009) 024422.
- [13] Z. Fisk, J.P. Remeika, in: K.A. Gshneidner, L. Eyring (Eds.), *Handbook on the Physics and Chemistry of Rare Earths*, vol. 12, Elsevier, North-Holland, Amsterdam, 1989, p. 53.
- [14] T.J.B. Holland, S.A.T. Redfern, *Mineral. Mag.* 61 (1997) 65.
- [15] P.G. Pagliuso, et al., *Phys. Rev. B* 62 (2000) 12266.
- [16] P.G. Pagliuso, et al., *J. Appl. Phys.* 99 (2006) 08P703.
- [17] P.G. Pagliuso, et al., *Phys. Rev. B* 63 (2001) 054426.
- [18] R. Lora-Serrano, et al., *Phys. Rev. B* 74 (2006) 214404.
- [19] K. Kato, et al., *Phys. Rev. Lett.* 84 (2000) 4204.
- [20] D. Stauffer, A. Aharony, *Introduction to Percolation Theory*, CRC Press, Boca Raton, FL, 1991.
- [21] T. Vojta, et al., *cond-mat/0707.0658*, 2008.